Multi-sensor Data Fusion Techniques for RPAS Navigation and Guidance

Subramanian Ramasamy
RMIT University

Roberto Sabatini
Khalifa University

Multi-sensor Data Fusion Techniques for RPAS Navigation and Guidance

Francesco Cappello, Subramanian Ramasamy and Roberto Sabatini
School of Aerospace, Mechanical and Manufacturing Engineering
RMIT University, Melbourne, VIC 3000, Australia
roberto.sabatini@rmit.edu.au

Abstract

Integrated Navigation and Guidance Systems (NGS) based only on satellite and other low-cost navigation sensors (e.g., Micro-Electro-Mechanical System (MEMS) based inertial sensors) cannot guarantee the Required Navigation Performance (RNP) in all flight phases of Remotely Piloted Aircraft Systems (RPAS). In this paper, a novel NGS for a small-to-medium size RPAS is presented, which is based on Global Navigation Satellite System (GNSS), Vision Based Navigation (VBN) and other low-cost avionics sensors. Additionally, Aircraft Dynamics Model (ADM) is used to compensate for the MEMS based Inertial Measuring Unit (IMU) sensor shortcomings in high-dynamics attitude determination tasks. Two multi-sensor architectures are compared that are based on an Extended Kalman Filter (EKF) and an Unscented Kalman Filter (UKF) approach for data fusion. The ADM measurements are pre-filtered by an UKF to increase the ADM attitude solution validity time. The EKF based VBN-IMU-GNSS-ADM (E-VIGA) system and the UKF based system (U-VIGA) performances are evaluated in a small RPAS integration scheme (i.e., AEROSONDE RPAS platform) by exploring a representative cross-section of this RPAS operational flight envelope. Additionally, an error covariance analysis is performed on the Aircraft Dynamics Filter (ADF) using Monte Carlo simulation. The position and attitude accuracy comparison shows that the E-VIGA and U-VIGA systems fulfill the relevant RNP criteria, including precision approach down to CAT-II.

Keywords: Remotely Piloted Aircraft Systems, Aircraft Dynamics Models, Extended/Unscented Kalman Filter, Low-Cost Sensors, Required Navigation Performance and Vision Based Navigation.

Introduction

Small- to medium-size Remotely Piloted Aircraft Systems (RPAS) are being proposed as alternatives to manned aircraft in an increasing number of civil, military and research applications. In particular, small RPAS have the ability of performing tasks with higher manoeuvrability and longer endurance and, additionally, they pose less risk to human lives and nature [1]. In order to integrate RPAS into the current and future non-segregated airspace, they will require enhanced navigational capabilities in order to meet the Required Navigational Performance (RNP) levels [2-4]. High-integrity airborne and ground-based integrated Navigation and Guidance Systems (NGS) that include fail-safe architecture designs are required to meet the RNP criteria. The selection of the navigation sensors is based on the requirements of low-cost, low-weight/low-volume sensors capable of providing the required level of performance in all flight phases of a small-to-medium size RPAS including high dynamics manoeuvres. Global Navigation Satellite System (GNSS) and Micro-Electro-Mechanical System (MEMS) based Inertial Measuring Unit (IMU) are a highly synergistic combination of navigation sensors capable of providing an accurate navigation state vector better than any standalone/single sensor. Vision Based Navigation (VBN) sensors are also used for precision approach and landing (i.e., the most demanding and potentially safetycritical flight phase). Aircraft Dynamics Model (ADM) is used as a virtual sensor and is essentially a knowledge-based module used to augment the navigation state vector [5, 6]. When processed with estimation techniques, the ADM predicts the RPAS flight dynamics (aircraft trajectory and attitude motion). This approach allows a reduction of cost, weight/volume and support requirements and, with the appropriate combination of sensors and integration algorithms, gives increased accuracy, continuity availability and integrity to the overall system [5, 6]. Multi-sensor data fusion is an effective way of optimizing large volumes of data and is implemented by combining information from multiple sensors to achieve inferences that are not feasible from a single sensor or source [7]. In the last three decades, the Extended Kalman Filter (EKF) has become the most widely used algorithm in numerous nonlinear estimation applications [8]. In comparison to the Unscented Kalman Filter (UKF), the EKF is difficult to manipulate (i.e. computationally intractable) due to derivation of the Jacobean matrices. Furthermore, the accuracy of the propagated mean and covariance is limited to first order Taylor series expansion, which is caused by its linearization process [9]. The UKF overcomes the limitations of the EKF by providing derivative-free higher-order approximations by approximating a Gaussian distribution rather than approximating an arbitrary nonlinear function. The UKF is more accurate and robust in navigation applications by also providing much better convergence characteristics. The UKF uses sigma points and a process known as Unscented Transform (UT) to evaluate the statistics of a nonlinear transformed random variable [9 and 12-16]. Our previous research activities [6, 10 and 11] presented the various sensor choices, data fusion methods and the overall implementation of the VBN/IMU/GNSS/ADM (VIGA) NGS architecture. In this paper, we propose an integrated NGS approach employing three state-of-the-art physical sensors: MEMS-IMU, GNSS and VBN sensors, as well as augmentation from ADM [5-7]. Additionally, in this paper the ADM is also used to compensate for the MEMS-IMU sensor shortcomings experienced in high-dynamics attitude determination tasks. The EKF and UKF are compared to evaluate the performance of the data fusion schemes in a low-cost, low-weight/low-volume Navigation and Guidance System (NGS) architecture.

Mathematical Model

The EKF is implemented to filter the incorrect VBN sensor results to provide the best Position, Velocity and Attitude (PVA) estimates. It is assumed that the motion model of the aircraft is disturbed by uncorrelated zero-mean Gaussian noise. The EKF measurement model is defined as:

$$z_k = H_k * x_k + v_k \tag{1}$$

where z_k is the measurement vector, H_k is the design matrix, x_k is the state vector, v_k is the measurement noise and k is the k^{th} epoch of time, t_k.

$$x_{k+1} = \Phi_{\mathrm{k}} * x_k + G_k * w_k \tag{2}$$

where x_{k+1} is the state vector at epoch $k+1$, Φ_{k} is the state transition matrix from epoch k to $k+1$, G_k is the shaping matrix and w_k is the process noise. If the body rates are assumed to be constant during the sampling interval, Δt and first order and higher order integrations are applied, then the state transition equations are as follows [8]:

$$\begin{bmatrix} \phi(k+1) \\ \theta(k+1) \\ \omega_x(k+1) \\ \omega_y(k+1) \\ \omega_z(k+1) \end{bmatrix} = \begin{bmatrix} \phi(k) + \Delta t(\dot{\phi}(k)) \\ \theta(k) + \Delta t(\dot{\theta}(k)) \\ \omega_x(k) \\ \omega_y(k) \\ \omega_z(k) \end{bmatrix} + \begin{bmatrix} \eta_\phi(k) \\ \eta_\theta(k) \\ \eta_{\omega_x}(k) \\ \eta_{\omega_y}(k) \\ \eta_{\omega_z}(k) \end{bmatrix} \tag{3}$$

where:

$$\dot{\phi}(k) = (\omega_x(k)\sin(\phi(k)) + \omega_y(k)\cos(\phi(k))\tan(\phi(k)) + \omega_z(k) \quad (4)$$

$$\dot{\theta}(k) = \omega_x(k)\cos(\phi(k)) - \omega_y(k)\sin(\phi(k)) \quad (5)$$

where θ is the pitch angle and ϕ is the roll angle. The prediction algorithm of the EKF estimates the state vector and computes the corresponding covariance matrix P_k from the current epoch to the next one using the state transition matrix characterizing the process model described by:

$$P_{k+1}^{-} = \Phi_{k+1} P_k^{+} \Phi_{k+1}^{T} + Q_k \quad (6)$$

where P_{k+1}^{-} represents a predicted value computed by the prediction equations and P_k^{+} represents the updated values obtained after the correction equations. The process noise at a certain epoch k is characterized by the covariance matrix, Q_k. The Kalman gain is used to quantify the influence of new information present in the innovation vector on the estimation of the state vector and can be considered as a weight factor. This gain is defined by:

$$K_{k+1} = P_{k+1}^{-} H_{k+1}^{T} [H_{k+1} P_{k+1}^{-} H_{k+1}^{T} + R_{k+1}]^{-1} \quad (7)$$

where R_{k+1} is the measurement noise covariance matrix. The state vector of the system described in terms of error in position, δr^n, velocity, δv^n and attitude, ϵ^n is given by:

$$x = \begin{bmatrix} \delta r^n \\ \delta v^n \\ \epsilon^n \end{bmatrix} \quad (8)$$

An UKF is implemented to increase the ADM validity time. The UKF is a recursive estimator and is based on unscented transformations in which unscented transforms are used for calculating the statistics of a random variable that goes through a nonlinear transformation [9 and 12-16]. The following algorithm is used for state estimation applications [16]. The initialisation of the UKF is performed based of the process model equations given by:

$$\hat{x}_0 = m[x_0] \quad (9)$$

$$P_0 = m[(x_0 - \hat{x}_0)(x_0 - \hat{x}_0)^T] \quad (10)$$

where $\hat{x}_0$ is the initial state vector estimate, m is the mean, x_0 is the initial state vector which incorporates the initial state of the ADM, P_0 is the initial state covariance matrix and T is the transposition of the matrix. The process model of the UKF is based upon a set of sigma points. The sigma points, χ_i are selected based on the mean and covariance of x_k. The sigma points are obtained by [16]:

$$P_{k-1} = \{diag(P_{k-1})\}^T \quad (11)$$

$$\chi_{k-1} = \left[\hat{x}_{k-1} \quad \hat{x}_{k-1} + \gamma\sqrt{P_{k-1}} \quad \hat{x}_{k-1} - \gamma\sqrt{P_{k-1}}\right] \quad (12)$$

where P computes the diagonal of state covariance matrix and results in the lower triangular matrix of the state covariance matrix P and γ is the control parameter of the dispersion distance from the mean estimate in the computation of the sigma point matrix, χ. After the sigma points are calculated, a time update for each time step $k = 1, 2,.., \mathrm{n}$ is performed and is given by [16]:

$$\chi_{k|k-1}^{*} = fn[\chi_{k-1}, u_{k-1}] \quad (13)$$

$$\hat{x}_k^{-} = \sum_{i=0}^{2L} W_i^{(m)} \chi_{i,k|k-1}^{*} \quad (14)$$

$$P_k^{-} = \sum_{i=0}^{2L} W_i^{(C)} [\chi_{i,k|k-1}^{*} - \hat{x}_k^{-}][\chi_{i,k|k-1}^{*} - \hat{x}_k^{-}]^T + R^v \quad (15)$$

$$^5\,\chi_{k|k-1} = \left[\hat{x}_k^{-} \quad \hat{x}_k^{-} + \gamma\sqrt{P_k^{-}} \quad \hat{x}_k^{-} - \gamma\sqrt{P_k^{-}}\right] \quad (16)$$

$$\mathcal{Y}_{k|k-1} = fn[\chi_{k|k-1}] \quad (17)$$

$$\hat{y}_k^{-} = \sum_{i=0}^{2L} W_i^{(m)} y_{i,k|k-1} \quad (18)$$

where χ_k represents the unobserved state of the system, u_k is a known exogenous input, W_i is a set of scalar weights that corresponds to each sigma point when it undergoes a nonlinear transformation at each iteration $i = 1, 2, \ldots, 2L$. R^v is the process noise covariance matrix, C in $W_i^{(C)}$ is the covariance and m in $W_i^{(m)}$ is the mean and L is the dimension of the augmented state vector. The measurement update equations are given by [16]:

$$P_{\tilde{y}_k \tilde{y}_k} = \sum_{i=0}^{2L} W_i^{(C)} \left[\mathcal{Y}_{i,k|k-1} - \hat{y}_k^-\right]\left[\mathcal{Y}_{i,k|k-1} - \hat{y}_k^-\right]^T + R^n \tag{19}$$

$$P_{x_k y_k} = \sum_{i=0}^{2L} W_i^{(C)} \left[\chi_{i,k|k-1} - \hat{x}_k^-\right]\left[\mathcal{Y}_{i,k|k-1} - \hat{y}_k^-\right]^T \tag{20}$$

$$\mathcal{K}_k = P_{x_k y_k} P_{\tilde{y}_k \tilde{y}_k}^{-1} \tag{21}$$

$$\hat{x}_k = \hat{x}_k^- + \mathcal{K}_k (y_k - \hat{y}_k^-) \tag{22}$$

$$P_k = P_k^- - \mathcal{K}_k P_{\tilde{y}_k \tilde{y}_k} \mathcal{K}_k^T \tag{23}$$

where R^n is the measurement noise covariance matrix [16]. The parameter y is the nonlinear function used for propagation of the sigma points, x_{k} is the k^{th} component of the vector x, $\hat{x}$ is an estimate of the value of x, $\hat{\mathrm{x}}_{\mathrm{k}}(-)$ is a-priori estimate of $\mathrm{x_n}$, conditioned on all priori measurements except the one at time $\mathrm{t_k}$, $\hat{\mathrm{x}}_{\mathrm{k}}(+)$ is a-posteriori estimate of $\mathrm{x_k}$, conditioned on all priori measurements at time $\mathrm{t_k}$. The UKF calculates the new sigma points every time in the time update and hence it requires the computation of a matrix square-root of the state covariance.

NGS Architectures

The two multi-sensor integrated NGS architectures compared are the EKF based VBN-IMU-GNSS-ADM (E-VIGA) and the UKF based system (U-VIGA). The E-VIGA architecture [6] uses VBN at 20 Hz and Global Positioning System (GPS) at 1 Hz to augment the MEMS-IMU running at 100 Hz. This architecture includes ADM (computations performed at 100 Hz) to provide attitude channel augmentation. The sensor measurements are handled by a sensor processing and data sorting block. The data sorting algorithm is based on Boolean decision logics, which allow automatic selection of the sensor data based on pre-defined priority criteria. The sorted data is then fed to an EKF to obtain the best estimate values. The INS position and velocity are compared with the GPS position and velocity to form the measurement input of the data fusion block containing the EKF. The attitude data provided by the ADM and the INS are compared to feed the EKF at 100 Hz, and the attitude data provided by the VBN sensors and INS are compared at 20 Hz and form the inputs to the EKF. The EKF provides estimates of Position, Velocity and Attitude (PVA) errors, which are then removed from the sensor measurements to obtain the corrected PVA states. The U-VIGA architecture is illustrated in Fig. 1. In this architecture, the EKF is replaced by an UKF. Additionally, an UKF is also used to pre-process the ADM navigation solution. The ADM operates differently to that of the VIGA system running in parallel to the centralised UKF and acts as a separate subsystem. The pre-filtering of the ADM virtual sensor measurements aids in achieving reduction of the overall position and attitude error budget and importantly considerable reduction in the ADM re-initialisation time. PVA measurements are obtained as state vectors from both the centralised UKF and ADM/UKF. These measurements are then fed into an error analysis module in which the measurement values of the two UKF are compared. The error analysis block includes the primary sensors (GNSS, INS and VBN) and it is used to compare the VIG error values with the virtual sensor (ADM) error values to obtain the corrected PVA states.

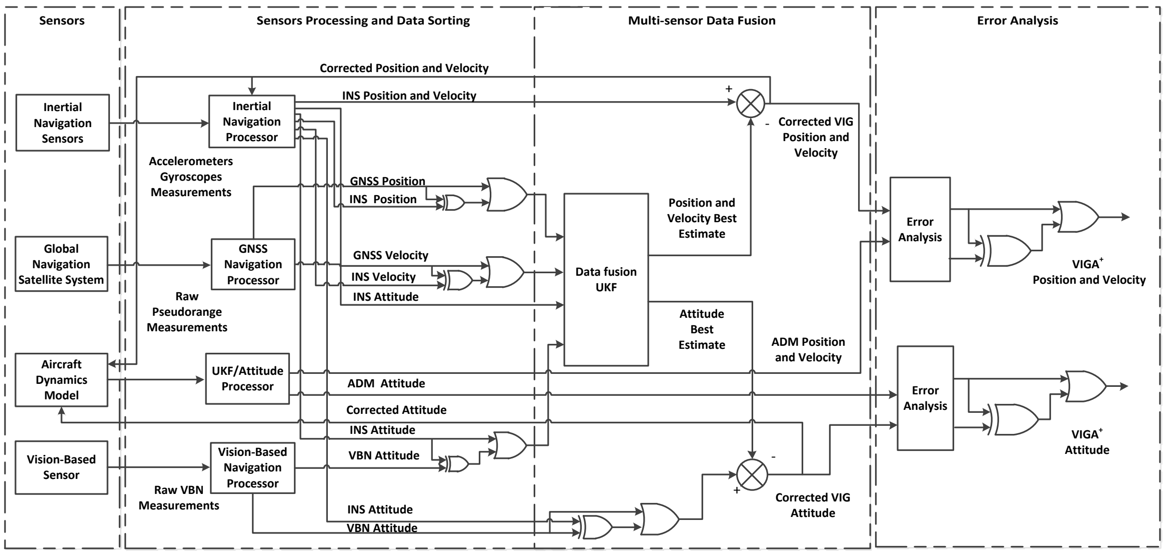

Fig. 1: U-VIGA architecture

Unscented Kalman Filter Performance Analysis

In practice, when a Kalman filter is used to estimate the system states, it also provides information about the accuracy of the estimates. The relevant information is embedded in the error covariance matrix, P. To extract the relevant information, a Monte Carlo simulation is performed in MATLAB™ and Simulink for 100 iterations with the duration of 10 seconds for each run. The performance analysis is performed on the pre-filtering UKF used in conjunction with the ADM. The simulation was set up using different noise seeds based on the specificities of the Monte Carlo technique. To analyse the performance of the UKF the computed error covariance P is compared with the mean errors. The performance of the filter is based on the condition that the mean and standard deviation errors are closer to zero and by evaluating $\sqrt{P_{diagonal}}$ values [18]. Fig. 2 illustrates the results of the error covariance analysis performed on the Aircraft Dynamics Filter (ADF).

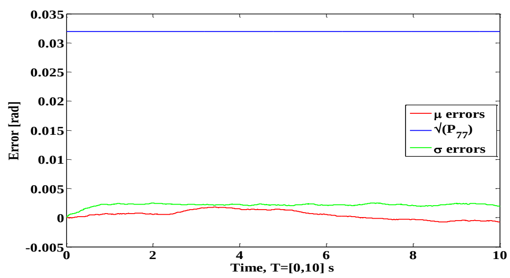

a. Phi

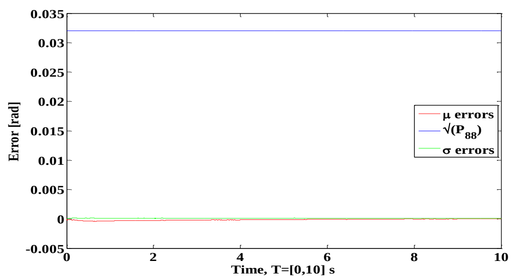

b. Theta

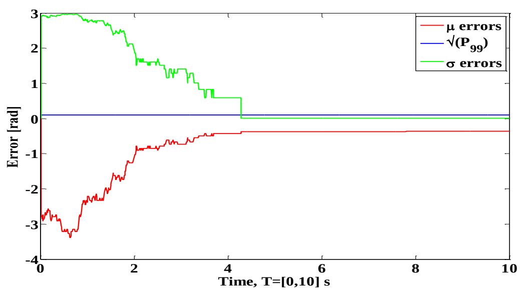

c. Psi

Fig. 2: U-VIGA Estimated Attitude Error Analysis

It is evident that the UKF does not diverge and the mean and standard deviation errors are close to zero. Additionally, Fig. 2c depicts a convergence in mean and standard deviation errors indicating that filter performance improves over time. The Monte Carlo simulation was performed by collecting data from several random runs and then by comparing the average values. Table 1 lists the mean, median and Standard Deviation (SD) values of the attitude errors. The steps adopted for evaluation were [18]:

- Taking the square root of diagonal terms of the process noise covariance matrix to obtain the theoretical estimation error of the standard deviation.
- The difference between the actual and estimated states was obtained from the actual estimation errors and compared with the error covariance matrix.

Table 1: ADF attitude statistics

ADF Statistics	Phi [rad]		Theta [rad]		Psi [rad]	
	μ_{errors}	σ_{errors}	μ_{errors}	σ_{errors}	μ_{errors}	σ_{errors}
Mean	0.0005	0.0022	-0.0001	0.0001	-0.8267	0.8006
Median	0.0006	0.0022	-0.0001	0.0001	-0.3698	0.0061
SD	0.0008	0.0003	0.0001	0.0000	0.8313	1.0844

Simulation Case Study

A detailed case study was performed in a high dynamics RPAS environment, employing a six-degree-of-freedom (6-DoF) model of the AEROSONDE RPAS as the reference ADM. The corresponding E-VIGA and U-VIGA integrated navigation modes were simulated using MATLAB™ in an appropriate sequence of flight manoeuvres representative of the AEROSONDE RPAS operational flight envelope. The duration of the simulation is 950 seconds covering eight flight legs (i.e., take off, straight climb, right climb helix, straight and level cruise, loiter, straight and level cruise, left descent helix, final straight approach) from starting point to destination. The 3D trajectory plot of the flight profiles of the AEROSONDE RPAS is illustrated in Fig. 3.

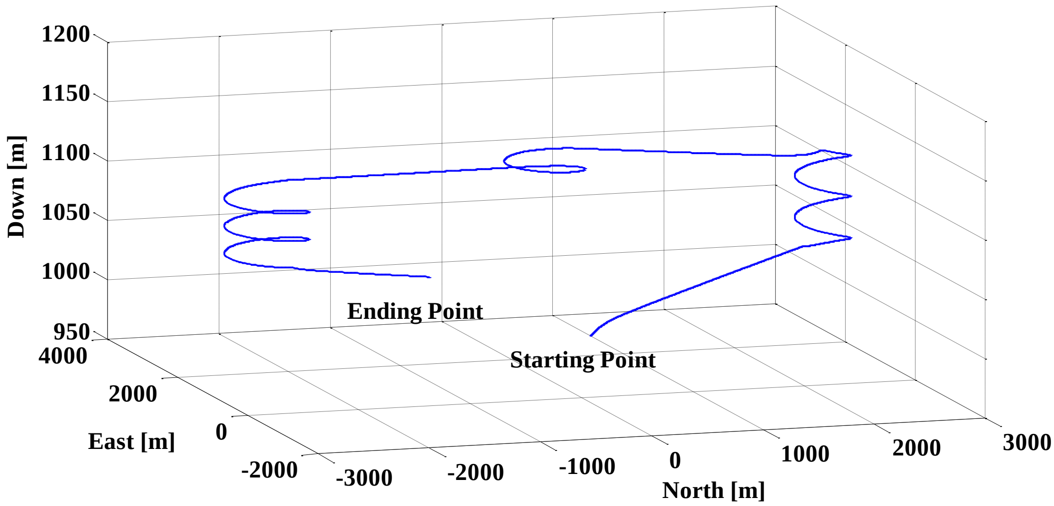

Fig. 3: 3D trajectory plot of RPAS flight profile

The best estimates of position, velocity and attitude for the two NGS architectures are obtained and the associated error statistics (mean, μ and standard deviation, σ) are calculated. Tables 2 and 3 list the position and attitude error statistics of the two NGS architectures respectively. The E-VIGA NGS system is prone to rapid divergence and its optimal time for re-initialisation is in the order of 20 seconds. The U-VIGA NGS system shows considerable improvement in the horizontal and vertical positions. By applying an UKF to pre-filter the ADM measurements, the navigational solution is corrected and becomes suitable for an extended time of operation. Comparing with the E-VIGA solution, a significant improvement of the solution validity time is obtained with the U-VIGA system as shown in Table 4. In particular, the lateral position validity time before the solution exceeds the RNP 1 threshold in the climb phase is 227 sec and, in the final approach phase, the ADM solution exceeds the CAT I, CAT II and CAT III limits at 151 sec, 144 sec and 46 sec respectively (the E-VIGA was compliant with RNP 1 threshold up to 110 sec, CAT I up to 107 sec, CAT II up to 64 sec and CAT III up to sec to 41 sec). The vertical position validity time before the solution exceeds the RNP 1 threshold in the climb phase is 200 sec. Furthermore, CAT II and CAT III requirements were satisfied up to 58 sec and CAT I requirements up to 116 sec. Table 5 lists a comparison of the E-VIGA and U-VIGA horizontal and vertical accuracy (RMS-95%) with the required accuracy levels for precision approach as recommended by the International Civil Aviation Organization [17] and the obtained results are in line with CAT II precision approach requirements.

Table 2: Position error statistics

NGS Architecture	North Position [m]		East Position [m]		Down Position [m]	
	μ	σ	μ	σ	μ	σ
E-VIGA	0.3673	2.0014	-0.4987	1.9445	0.1776	2.4524
U-VIGA	0.4793	1.4062	-0.4064	1.7339	0.1211	2.2581

Table 3: Attitude error statistics

NGS Architecture	Pitch (θ) [degrees]		Roll (ϕ) [degrees]		Heading (ψ) [degrees]	
	μ	σ	μ	σ	μ	σ
E-VIGA	0.0055	0.0407	-0.0069	0.3140	-0.0017	0.0449
U-VIGA	0.0051	0.0400	-0.0053	0.2197	0.0010	0.0417

Table 4: E-VIGA and U-VIGA ADM lateral and vertical guidance validity times

Accuracy threshold	ADM validity time [sec]			
	Lateral Position		Vertical Position	
	E-VIGA	U-VIGA	E-VIGA	U-VIGA
RNP 1	110	227	95	200
CAT I	107	151	62	116
CAT II	64	144	19	58
CAT III	41	46		

Table 5: E-VIGA and U-VIGA position error statistics (precision approach)

Category of approach	Horizontal Accuracy [m] 2D RMS - 95%			Vertical Accuracy [m] RMS - 95% Down		
	Required	E-VIGA	U-VIGA	Required	E-VIGA	U-VIGA
CAT I	16	5.2	4.8	4	1.9	1.9
CAT II	6.9			2		
CAT III	4.1			2		

Conclusion

The research activities performed to design a low-cost and low-weight/volume integrated NGS suitable for small-to-medium size RPAS applications were described. Various sensors were considered for the NGS design including GNSS and MEMS-IMU, with augmentation from ADM and VBN sensors. Two different low-cost and low-weight/volume integrated NGS architectures were introduced. They are the EKF based E-VIGA integrated system and the

UKF based U-VIGA system. While the E-VIGA system uses unfiltered ADM data, the U-VIGA system employs an UKF for pre-filtering the ADM attitude solution and thus increases the ADM solution validity time. Simulation of the E-VIGA integrated navigation mode showed that the integration schemes can achieve horizontal/vertical position accuracies, with a significant improvement compared to stand-alone GNSS and integrated GNSS/INS. Compared to the E-VIGA system, the U-VIGA system showed an improvement of accuracy in the position and attitude measurements in addition to an increased ADM validity time. Furthermore, the performance of the UKF processing attitude channel data from the ADM was validated with a Monte Carlo simulation. Additionally, the integration schemes achieved horizontal/vertical position accuracies in line with CAT-II precision approach requirements. Future research will address uncertainty analysis and possible synergies of the E-VIGA and U-VIGA architectures with GNSS avionics based integrity augmentation systems.

References

1. Laliberte, A.S., Rango, A. and Herrick, J.E., "Unmanned Aerial Vehicles for Rangeland Mapping and Monitoring: A Comparison of Two Systems", *Proceedings of the ASPRS Annual Conference*, Tampa, Florida, USA, 2007.
2. Lacher, A, et al., "Airspace Integration Alternatives for Unmanned Aircraft", *Center for Advanced Aviation System Development, The MITRE Corporation*, 2010.
3. DeGarmo, M.T. and Nelson, G.M., "Prospective Unmanned Aerial Vehicle Operations in the Future National Airspace System", *AIAA 4th Aviation Technology, Integration and Operations (ATIO) Forum*, 2004.
4. DeGarmo, M.T., "Issues Concerning Integration of Unmanned Aerial Vehicles in Civil Airspace", *The MITRE Corporation*, McLean, Virginia, 2004.
5. Cork, L.R., "Aircraft Dynamic Navigation for Unmanned Aerial Vehicles", Thesis, Queensland University of Technology, 2014.
6. Sabatini, R., Ramasamy, S., Gardi, A. and Rodríguez, L., "Low-cost Sensors Data Fusion for Small Size Unmanned Aerial Vehicles Navigation and Guidance", *International Journal of Unmanned Systems Engineering*, Vol. 1, No. 3, pp. 16-47, 2013. DOI: 10.14323/ijuseng.2013.11.
7. Jiang, D, et al., "Advances in Multi-Sensor Data Fusion: Algorithms and Applications", *Journal of Sensors*, Vol. 9, Issue. 10, 2009, pp. 7771-7784.
8. Ribeiro, M.I., "Kalman and Extended Kalman Filters: Concept, Derivation and Properties", *Institute for Systems and Robotics,* 2004.
9. Julier, S.J. and Uhlman, J.K., "A New Extension of the Kalman Filter to Nonlinear Systems", *International Symposium of Aerospace/defense Sensing, Simulation and Controls*, Vol. 3, No. 26, 1997.
10. Sabatini, R., Cappello, F., Ramasamy, S., Gardi, A. and Clothier, R., "An Innovative Navigation and Guidance System for Small Unmanned Aircraft using Low-Cost Sensors", *Journal of Aircraft Engineering and Aerospace Technology*, 2015. (In press)
11. Sabatini, R., Ramasamy, S., Cappello F. and Gardi, A., "RPAS Navigation and Guidance Systems based on GNSS and other Low-Cost Sensors," *Fourth Australasian Unmanned Systems Conference 2014 (ACUS 2014),* Melbourne, Australia. DOI: 10.13140/2.1.3792.8008
12. Julier, S.J., Uhlman, J.K. and Durrant, W.H., "A New Approach for Filtering Nonlinear Systems", *Proceedings of the 1995* IEEE *American Control Conference,* Vol. 3, 1995.
13. Merwe, R.v.d., "Sigma-point Kalman filters for Probabilistic Inference in Dynamic State-Space Models", Dissertation, *Oregon Health & Science University*, 2004.

14. Merwe, R.v.d., Wan, E.A. and Julier, S.J., "Sigma-point Kalman Filters for Nonlinear Estimation and Sensor-Fusion: Applications to Integrated Navigation", *Proceedings of the AIAA Guidance, Navigation & Control Conference*, 2004.
15. Wan, E.A. and Merwe, R.v.d., "The Unscented Kalman Filter for Nonlinear Estimation", *Proceedings of Symposium 2000 on Adaptive Systems for Signal Processing, Communication and Control (AS-SPCC)*, Lake Louise, Alberta, Canada, 2000.
16. Merwe, R.v.d. and Wan, E.A., "The Square-Root Unscented Kalman Filter for State and Parameter-Estimation", *Proceedings of the IEEE International Conference on Acoustics, Speech, and Signal Processing (ICASSP'01)*, Vol. 6. IEEE, 2001.
17. ICAO, "Annex 10 to the Convention on International Civil Aviation, Aeronautical Telecommunications - Volume 1: Radio Navigation Aids", 6th edition, 2006.
18. Rapid STM32 Team, "Developing a Tilt Sensor System using Rapid STM32 Blockset", Vol. 1, Application note.